Community Assembly and Environmental Filtering Along a Disturbance–Climate Gradient in a Himalayan Tiger Landscape

Wangdi[1] & Rupesh Subedi[2]
[1] Forest Resources Planning and Management Division, Department of Forests and Park Services, Royal Government of Bhutan
[2] College of Natural Resources, Royal University of Bhutan

Abstract

Understanding the processes that structure wildlife communities is central to biodiversity conservation; however, disentangling the relative roles of environmental filtering and biotic interactions remains methodologically challenging in species-rich tropical and subtropical systems. This study analysed camera-trap data from 149 stations (12,835 trap-nights) distributed across a contiguous protected-area network in south-central Bhutan, encompassing Royal Manas National Park, Phipsoo Wildlife Sanctuary, and Sarpang Forest Division. The objective was to quantify the relative contributions of climatic gradients, anthropogenic disturbance, and interspecific interactions to mammalian community assembly along an elevational gradient ranging from 64 to 2,552 m. Non-metric multidimensional scaling (NMDS) indicated that climatic variables were the primary determinants of community composition. Annual precipitation (BIO12; $r^2 = 0.366$, $p = 0.001$) and mean annual temperature (BIO1; $r^2 = 0.311$, $p = 0.001$) exhibited the strongest associations with species turnover, whereas distance to roads exerted a weaker but statistically significant effect ($r^2 = 0.052$, $p = 0.014$). Probabilistic co-occurrence analysis identified 214 significant species pairs out of 990 tested (21.6%), comprising 143 positive and 71 negative associations. These relationships persisted after controlling shared habitat preferences, indicating the presence of residual biotic structuring beyond environmental filtering. Cluster analysis ($k = 2$; average silhouette width = 0.128) differentiated two principal assemblages along the elevational gradient. Highland communities were characterised by species such as the yellow-throated marten and marbled cat, whereas lowland assemblages were dominated by Asian elephant and tiger. Despite spatial co-occurrence between apex predators and subordinate carnivores, no evidence of mesopredator release was detected (tiger–leopard: $r = -0.07$, $p > 0.05$; tiger–dhole: $r = -0.17$, $p = 0.084$). Species accumulation curves approached an asymptote by 149 stations, with a total of 73 species recorded, indicating sufficient sampling completeness. Collectively, these findings demonstrate that climatic gradients constitute the dominant assembly filter in this Himalayan landscape, while anthropogenic disturbance exerts a secondary but detectable influence. Residual co-occurrence patterns further suggest the operation of biotic interactions, warranting future investigation using integrative frameworks such as joint species distribution models.

Keywords: camera trapping, community assembly, co-occurrence, environmental filtering, NMDS ordination, species interactions, tropical mammals, wildlife community

Introduction

The processes governing community assembly – environmental filtering, biotic interactions, and dispersal limitation – operate simultaneously across spatial scales, making their disentanglement one of the central challenges in community ecology (HilleRisLambers et al., 2012; Kraft et al., 2015). Environmental filtering theory predicts that abiotic conditions select for species with traits suited to local conditions, generating predictable associations between community composition and environmental gradients (Cavender-Bares et al., 2009). In terrestrial mammalian communities, temperature and precipitation gradients impose broad-scale constraints on species distributions and assemblage structure, particularly along elevational transects where climatic variables change rapidly over short distances (Blois et al., 2013; Chen et al., 2011).

Anthropogenic disturbance introduces a second filtering mechanism that can override or interact with climatic structuring. Roads, settlements, and land-use conversion reduce habitat quality and connectivity, disproportionately affecting species with large home ranges, low reproductive rates, and high sensitivity to human activity (Benitez-Lopez et al., 2010; Newbold et al., 2015). A global synthesis demonstrated that vertebrate assemblages within 5 km of roads harbour 15–25% fewer species than undisturbed areas, with large carnivores exhibiting the strongest negative responses (Benitez-Lopez et al., 2010). Understanding how disturbance gradients filter community composition relative to climate is essential for conservation planning, particularly in regions where development pressures are intensifying within or adjacent to protected areas.

Beyond environmental filtering, biotic interactions shape community structure through competition, predation, and facilitation. Species co-occurrence patterns – the degree to which species are found together more or less frequently than expected by chance – provide a widely used proxy for inferring biotic interactions from observational data (Gotelli, 2000; Veech, 2013). Null model approaches that compare observed co-occurrence matrices against randomised expectations can identify species pairs whose spatial associations deviate significantly from habitat-driven predictions, potentially reflecting competitive exclusion, predator avoidance, or mutualistic facilitation (Blanchet et al., 2020). However, interpreting co-occurrence patterns requires caution, as shared or divergent habitat preferences can generate spurious signals of interaction (Ovaskainen et al., 2017).

Camera-trap surveys have transformed the study of terrestrial mammal communities by enabling simultaneous monitoring of multiple species across large spatial extents without the taxonomic or habitat biases inherent in visual encounter surveys (Ahumada et al., 2011; Rovero et al., 2014). When deployed at sufficient station density with standardised effort, camera-trap networks yield community-level detection data suitable for ordination, co-occurrence analysis, and diversity estimation (Tobler et al., 2008; Sollmann, 2018). The relative abundance index (RAI), calculated as detections per unit survey effort, provides a standardised metric for comparing species composition across stations, although its interpretation as a density surrogate requires assumptions about detection probability that may not hold uniformly across species (Sollmann, 2018).

Guild-specific responses to environmental gradients provide additional insight into assembly mechanisms. Large carnivores, with their extensive spatial requirements and sensitivity to human disturbance, are expected to show stronger filtering responses than smaller-bodied guilds (Cardillo et al., 2005; Ripple et al., 2014). Ungulates may respond more strongly to vegetation

productivity gradients that determine forage availability, while small carnivores and mesopredators may exhibit complex responses mediated by both habitat and intraguild interactions. The mesopredator release hypothesis predicts that subordinate carnivores increase in abundance when apex predators are reduced or absent (Soule et al., 1988; Prugh et al., 2009). Testing this prediction in landscapes where apex predators persist at ecologically effective densities provides a valuable contrast to the degraded systems in which mesopredator release has been most commonly documented (Ritchie & Johnson, 2009).

South-central Bhutan presents an ideal study system for investigating community assembly along coupled disturbance–climate gradients. The region encompasses a contiguous forest corridor spanning 64–2,552 m elevation within Royal Manas National Park, Phipsoo Wildlife Sanctuary, and Sarpang Forest Division, supporting a diverse mammalian assemblage that includes large apex predators (tiger, leopard, dhole), large ungulates (gaur, sambar, Asian elephant), and a rich mesocarnivore guild (Tempa et al., 2019; Penjor et al., 2021). Bhutan's extensive forest cover (>70% of national area) and low human population density within protected areas provide a comparatively undisturbed context in which to study assembly processes closer to their natural baseline (Wang et al., 2015).

Six research questions were formulated to evaluate the drivers of community assembly across disturbance and climatic gradients. First, the independent effect of anthropogenic disturbance (road proximity and building density) on community composition was tested, with the expectation that these variables would emerge as significant environmental vectors in multivariate ordination space after accounting for climatic influences. Second, differential sensitivity of trophic guilds was assessed by comparing carnivores and ungulates along disturbance gradients, with the prediction that carnivores would exhibit stronger negative responses. Third, the persistence of residual species associations was evaluated after controlling shared habitat responses, with the expectation that a substantial proportion of significant co-occurrence pairs would remain beyond environmental expectations. Fourth, the relative strength of climatic variables, including temperature, total precipitation, and precipitation seasonality, was quantified as drivers of community structure, with precipitation hypothesised to represent the dominant gradient due to the pronounced monsoonal regime in the region. Fifth, the presence of mesopredator release was tested by examining correlations between apex predator and subordinate carnivore abundances, with the expectation that no release signal would be detected in a system where tiger populations persist at moderate densities. Sixth, sampling adequacy was assessed using species accumulation curves and richness estimators, with the prediction that sampling coverage would approach asymptotic completeness at 149 camera-trap stations.

Methods

Study area

The study was conducted across three contiguous protected areas in south-central Bhutan: Royal Manas National Park (RMNP; 1,057 km^2), Phipsoo Wildlife Sanctuary (PWS; 278 km^2), and Sarpang Forest Division (SFD), collectively spanning the southern foothills of the eastern Himalayas (Figure 1). The landscape encompasses subtropical broadleaf and mixed coniferous forests along a steep elevational gradient (64–2,552 m a.s.l.), dissected by major river systems. The region experiences a monsoonal climate with wet (June–September) and dry (November–March) seasons. Mean annual temperature across stations ranged from 18.1 to 23.1 degrees C

(BioClim bio1), annual precipitation from 2,293 to 4,543 mm (bio12), and precipitation seasonality from 107.9 to 113.5 (bio15 coefficient of variation). Land use is predominantly forested, with scattered agricultural settlements along river valleys.

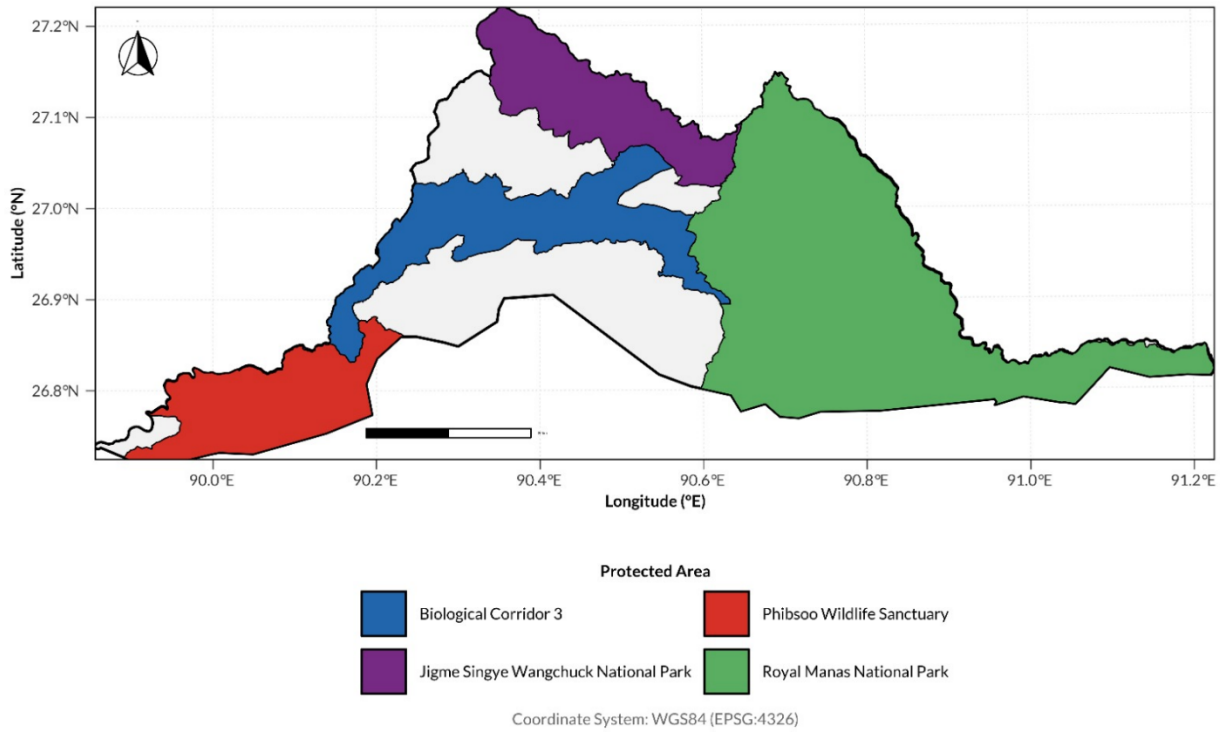

Figure 1: Map of Study Area: South Central Bhutan.

Camera-trap survey design and effort

A total of 149 camera-trap stations were deployed between January and December 2022, yielding 12,835 trap-nights (range per station: 41–350 days). Stations were systematically positioned along wildlife trails, ridge lines, and riparian corridors to maximise detection probability across habitat types. Each station comprised paired cameras mounted at approximately 40 cm above ground level. Inter-station spacing averaged ~2 km to reduce spatial autocorrelation while maintaining landscape coverage. Independent detection events were defined using a 20-minute threshold within each species–station combination to minimise pseudo-replication (O'Brien et al., 2003; Meek et al., 2014).

Community matrix construction

A species-by-station community matrix was constructed using the relative abundance index (RAI), calculated as the number of independent detections per 100 trap-nights at each station. Species recorded at fewer than five stations were excluded to reduce the influence of rare taxa on multivariate analyses, resulting in a 42-species × 149-station matrix. Human detections (1,356 events across all stations) were excluded from the community matrix but retained as an environmental predictor. Species were assigned to functional guilds (carnivore, ungulate, primate, bird, rodent, reptile, pangolin) based on established dietary and taxonomic classifications.

NMDS ordination and environmental fitting

Community composition was analysed using non-metric multidimensional scaling (NMDS) based on Bray–Curtis dissimilarity, implemented via the metaMDS function in the vegan package (Oksanen et al., 2022). Two ordination dimensions (k = 2) were specified, with 100 random starts to avoid convergence on local minima. Ordination quality was assessed using stress, with values < 0.20 considered acceptable for ecological community data (Clarke, 1993).

Environmental drivers of community structure were evaluated using the envfit function, which fits environmental vectors to ordination space and assesses significance via permutation tests (999 permutations). Seven predictors included: latitude, longitude, sampling effort (trap-nights), distance to nearest road (m), mean annual temperature (BIO1, °C), annual precipitation (BIO12, mm), and precipitation seasonality (BIO15, coefficient of variation). Climatic variables were extracted from WorldClim v2.1 at 250 m resolution (Fick & Hijmans, 2017), while road distance was derived from a GeoPackage-based road network. Vector strength was quantified using the coefficient of determination (r^2), with significance assessed via permutation-derived p-values.

Species co-occurrence analysis

Non-random species co-occurrence patterns were evaluated using a probabilistic null model framework. For each of 990 pairwise combinations among 45 species with sufficient detections, observed co-occurrence frequencies were compared to expectations under a null model preserving species-specific occurrence frequencies. Standardised effect sizes (SES) were computed as:

$$SES = (observed - expected) / SD\ (expected)$$

Species pairs with |SES| > 1.96 were classified as significantly positive (SES > 1.96) or negative (SES < −1.96) at $\alpha = 0.05$ (Gotelli, 2000; Veech, 2013).

Station clustering and indicator species analysis

Hierarchical clustering of stations was conducted using Bray–Curtis dissimilarity and Ward's minimum variance method. The optimal number of clusters was determined by maximising the average silhouette width across k = 2–10. Indicator species associated with each cluster were identified using the IndVal index (Dufrêne & Legendre, 1997), implemented in the indicspecies package, with significance assessed via 999 permutations.

Activity overlap analysis

Diel temporal overlap between species pairs was quantified using the $\hat{\Delta}_4$ coefficient of overlap (Ridout & Linkie, 2009; Meredith & Ridout, 2014), producing a 42 × 42 symmetric overlap matrix. Species were ordered by functional guild to facilitate interpretation of within- and between-guild temporal partitioning.

Land-cover analysis

Each station was assigned to the nearest land-cover class from a 2020 land-use/land-cover (LULC) dataset within a GeoPackage spatial database using st_nearest_feature in the sf package (Pebesma, 2018). Mean RAI was calculated for each guild–LULC combination to assess patterns of habitat use across functional groups.

Climate–diversity relationships

Relationships between climatic variables (BIO1, BIO12, BIO15) and station-level species richness and total RAI were evaluated using Pearson correlation coefficients and visualised using LOESS smoothing. Climatic predictors were extracted at 250 m resolution from WorldClim bioclimatic layers.

Mesopredator release test

Mesopredator release was assessed by correlating $\log_{1+}$-transformed RAI of the apex predator (tiger) with subordinate carnivores (common leopard and dhole) across stations where both taxa were detected. Pearson correlation coefficients and associated p-values were computed. Stations with fewer than 30 trap-nights were excluded to minimise bias from short sampling durations.

Species accumulation and richness estimation

Sampling completeness was evaluated using a randomised species accumulation curve generated by iteratively adding stations in random order (1,000 permutations) and recording cumulative species richness. The Chao1 estimator was calculated to estimate total local richness, accounting for undetected species based on singleton and doubleton frequencies (Chao, 1984; Colwell et al., 2012).

Software and reproducibility

All analyses were conducted in R version 4.4.0 within a reproducible target's workflow, with package dependencies managed using renv. Key packages included vegan (Oksanen et al., 2022), overlap (Meredith & Ridout, 2014), indicspecies (De Cáceres & Legendre, 2009), sf (Pebesma, 2018), and betareg (Cribari-Neto & Zeileis, 2010). Random processes were controlled using a fixed seed (set.seed(42)). The complete analytical pipeline is publicly available at: https://github.com/wangdiues/camtrap_ecology_analytics.

Results

Community overview

The camera-trap survey detected 73 species across 149 stations and 12,835 trap-nights. After applying the minimum 5-station detection threshold, 42 species were retained for community analysis. The most widely detected species were barking deer (*Muntiacus muntjak*; 145 stations, 3,168 detections), sambar (*Rusa unicolor*; 113 stations, 2,966 detections), gaur (*Bos gaurus*; 105 stations, 2,594 detections), and wild boar (*Sus scrofa*; 110 stations, 858 detections). Tigers (*Panthera tigris*) were detected at 51 stations (183 detections) and common leopard (*Panthera pardus*) at 72 stations. Station-level species richness ranged from 3 to 25 species (mean = 13.4, SD = 4.1), and total RAI ranged from 17.4 to 821.9 detections per 100 trap-nights (Table 1).

Table 1. Survey summary for the seven most widely detected focal species. Detections are independent events after applying a 20-minute filter. Station coverage is the proportion of 149 stations at which the species was detected. Mean group size is the average number of individuals per detection event.

Species	Detections	Stations	Coverage	Mean group size
Barking Deer	3,168	145	0.973	14.1
Sambar	2,966	113	0.758	21.6
Gaur	2,594	105	0.705	40.7
Asian Elephant	1,594	92	0.617	43.0
Wild Boar	858	110	0.738	16.1
Common Leopard	–	72	0.483	–
Tiger	183	51	0.342	–

NMDS ordination and environmental gradients

NMDS ordination converged on a two-dimensional solution with a stress value of 0.208, indicating an acceptable representation of community dissimilarity structure (Clarke, 1993). Environmental vector fitting revealed that climate variables were the strongest correlates of community composition (Table 2, Figure 2). Annual precipitation (bio12) exhibited the highest explanatory power (r^2 = 0.366, p = 0.001), followed by mean annual temperature (bio1; r^2 = 0.311, p = 0.001) and precipitation seasonality (bio15; r^2 = 0.075, p = 0.006). Among non-climatic variables, latitude (r^2 = 0.344, p = 0.001) and trap-nights (r^2 = 0.369, p = 0.001) were strongly associated with ordination axes, while distance to nearest road showed a weaker but significant association (r^2 = 0.052, p = 0.014). Longitude was not significantly correlated with community composition (r^2 = 0.015, p = 0.332).

Table 2. Environmental vector fitting (envfit) results from NMDS ordination of mammalian community composition across 149 camera-trap stations. NMDS1 and NMDS2 are the direction cosines of each vector; r^2 is the coefficient of determination from permutation tests (999 permutations). Variables are ordered by r^2.

Variable	NMDS1	NMDS2	r^2	p-value
Trap-nights	0.799	-0.601	0.369	0.001
Annual precipitation (bio12)	-0.395	-0.919	0.366	0.001
Latitude	0.451	0.892	0.344	0.001
Mean annual temperature (bio1)	-0.370	-0.929	0.311	0.001
Precipitation seasonality (bio15)	-0.315	-0.949	0.075	0.006
Distance to road (m)	-0.437	-0.899	0.052	0.014
Longitude	-0.305	-0.952	0.015	0.332

The envfit vectors for bio1, bio12, and dist_road_m were all oriented toward negative NMDS2 values, indicating that stations with higher temperatures, greater precipitation, and closer road proximity harboured distinct community assemblages from cooler, drier, more remote stations. The strong colinearity between bio1 and bio12 reflects the coupling of temperature and precipitation along the elevational gradient.

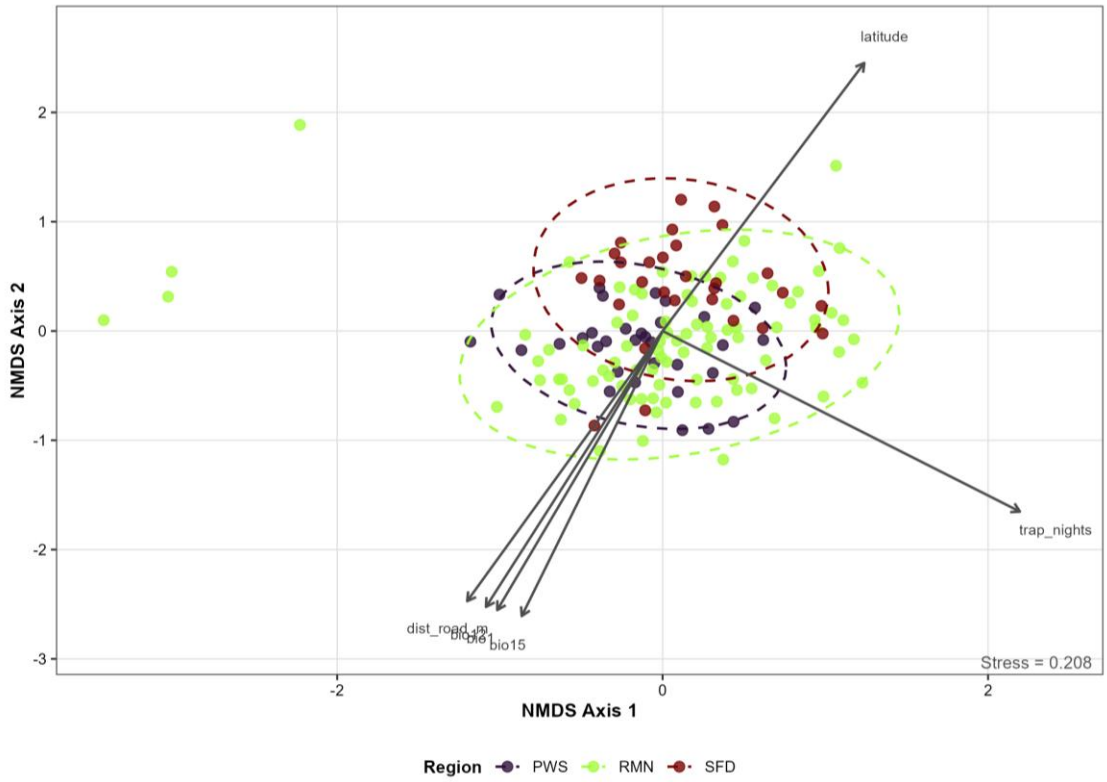

Figure 2. *Non-metric multidimensional scaling (NMDS) ordination of mammalian community composition across 149 camera-trap stations in south-central Bhutan (stress = 0.208). Each point represents one station, coloured by cluster membership (k = 2). Environmental vectors from envfit analysis are overlaid; vector length is proportional to* r^2*. Climate variables (bio1, bio12) and latitude are the dominant structuring forces, with distance to road exerting a weaker but significant effect.*

Species co-occurrence patterns

Probabilistic co-occurrence analysis of 990 pairwise species combinations identified 214 significant associations (21.6%), comprising 143 positive (14.4%) and 71 negative (7.2%) pairs (Figure 3). The strongest positive associations involved species sharing lowland habitats: Asian elephant–tiger (SES = 6.14), Asian elephant–gaur (SES = 5.77), masked palm civet–black stork (SES = 8.48), and black stork–tawny fish owl (SES = 7.85). These pairs co-occurred at substantially more stations than expected under the null model, suggesting shared habitat preferences or facilitative interactions (Table 3).

The strongest negative associations involved elevational segregation between lowland and highland species: Himalayan palm civet showed significant negative co-occurrence with Asian elephant (SES = -4.63), kalij pheasant with bird sp. (SES = -5.47), and Asian elephant with marbled cat (SES = -4.37). These negative associations are consistent with environmental filtering along the elevational gradient, where highland species (marbled cat, Himalayan palm civet, yellow-throated marten) occupy cooler, wetter habitats that are largely exclusive of lowland megafauna.

Table 3. Top 10 positive and top 10 negative co-occurrence pairs ranked by absolute SES value. Obs = observed number of stations with co-occurrence; Exp = expected under null model.

Species 1	Species 2	Obs	Exp	SES	Direction
Masked Palm Civet	Black Stork	5	0.3	8.48	Positive
Black Stork	Tawny Fish Owl	5	0.4	7.85	Positive
Large Indian Civet	Tawny Fish Owl	7	1.0	6.73	Positive
Red Junglefowl	Indian Peafowl	8	1.2	6.65	Positive
Large Indian Civet	Black Stork	7	1.2	6.30	Positive
Asian Elephant	Tiger	49	31.5	6.14	Positive
Red Junglefowl	Tawny Fish Owl	6	0.9	5.98	Positive
Asian Elephant	Gaur	81	64.8	5.77	Positive
Crab-eating Mongoose	Red Junglefowl	15	4.8	5.75	Positive
Common Palm Civet	Crab-eating Mongoose	20	8.1	5.64	Positive
Kalij Pheasant	Bird sp.	2	15.2	-5.47	Negative
Asian Elephant	Himalayan Palm Civet	11	22.2	-4.63	Negative
Asian Elephant	Marbled Cat	6	16.1	-4.37	Negative
Red Junglefowl	Bird sp.	1	9.8	-4.29	Negative
Gaur	Himalayan Palm Civet	16	25.4	-4.09	Negative
Blue Whistling Thrush	Bird sp.	0	5.4	-3.61	Negative
Himalayan Palm Civet	Civet sp.	0	8.0	-3.60	Negative
Indian Peafowl	Bird sp.	0	5.4	-3.46	Negative
Asian Elephant	Yellow-throated Marten	26	35.8	-3.34	Negative
Common Palm Civet	Civet sp.	0	6.6	-3.28	Negative

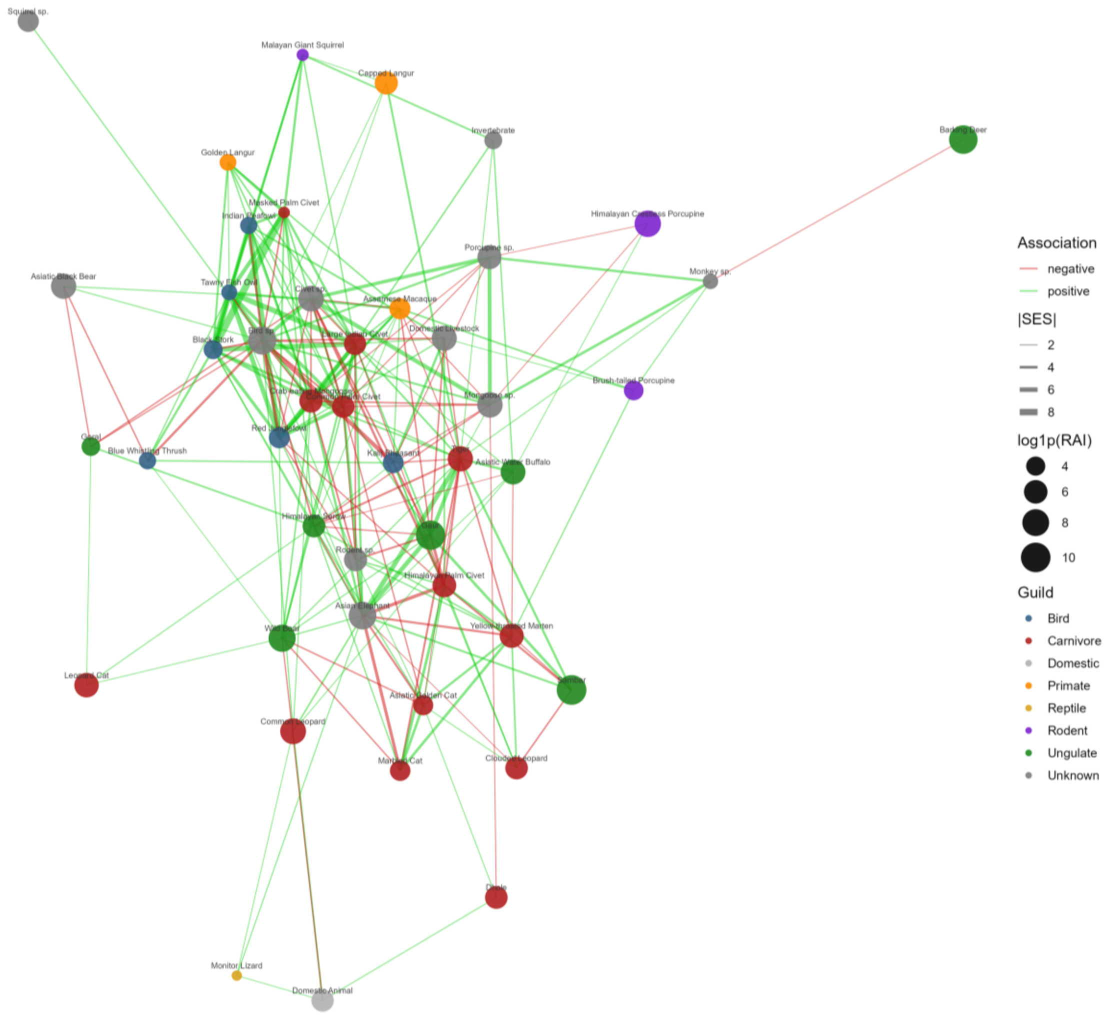

Figure 3. *Species co-occurrence network showing significant pairwise associations (|SES| > 1.96) among 42 mammal species. Green edges indicate positive associations (co-occurrence more frequent than expected); red edges indicate negative associations. Node size is proportional to the number of stations at which each species was detected. The network reveals a central cluster of lowland species (elephant, tiger, gaur) with strong positive associations, and a peripheral cluster of highland species with negative associations to the lowland assemblage.*

Station clustering

Hierarchical clustering identified an optimal partition of k = 2 clusters (average silhouette width = 0.128; Figure 7). The low silhouette value indicates that station-level community composition varies along a continuous gradient rather than forming discrete assemblage types. Nonetheless, indicator species analysis revealed ecologically interpretable cluster identities (Table 4). Cluster 1 was characterised by highland-associated species: yellow-throated marten (IndVal = 0.666, p = 0.001), Himalayan palm civet (IndVal = 0.615, p = 0.001), and marbled cat (IndVal = 0.566, p = 0.001). Cluster 2 was characterised by lowland megafauna: Asian elephant (IndVal = 0.801, p = 0.001), tiger (IndVal = 0.668, p = 0.001), and common palm civet (IndVal = 0.510, p = 0.001).

Table 4. Indicator species for each station cluster (k = 2), identified using the IndVal index. Only species with IndVal > 0.50 and $p < 0.01$ are shown.

Species	Cluster	IndVal	*p*-value
Asian Elephant	2	0.801	0.001
Tiger	2	0.668	0.001
Yellow-throated Marten	1	0.666	0.001
Himalayan Palm Civet	1	0.615	0.001
Marbled Cat	1	0.566	0.001
Common Palm Civet	2	0.510	0.001

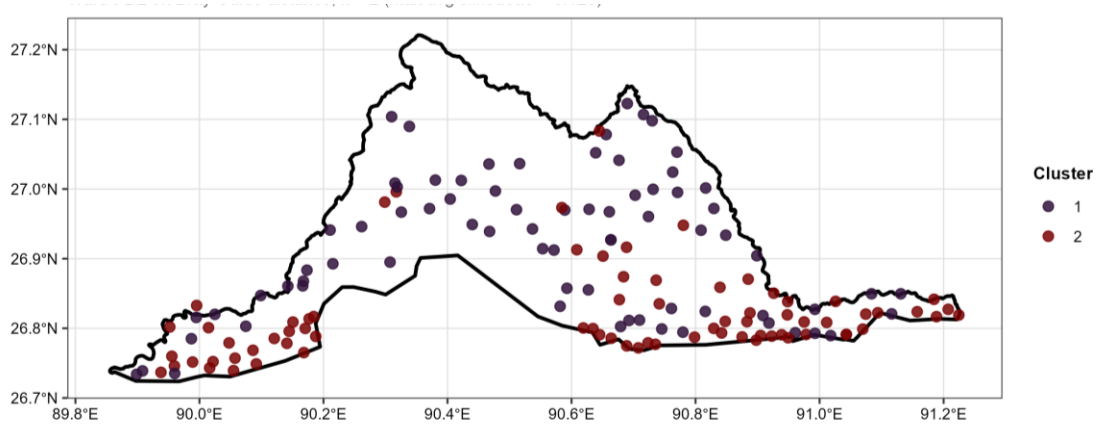

Figure 7. *Spatial distribution of station cluster membership (k = 2) across the study area. Cluster 1 (highland assemblage) stations are characterised by yellow-throated marten, Himalayan palm civet, and marbled cat. Cluster 2 (lowland assemblage) stations are dominated by Asian elephant, tiger, and common palm civet. The cluster boundary broadly follows the elevational gradient.*

Guild-specific habitat associations

Mean RAI varied substantially across LULC classes and guilds (Table 5, Figure S2). Forest habitats supported the highest species diversity, with carnivores (mean RAI = 8.99), ungulates (35.45), and primates (3.65) all showing highest detection rates in forested landscapes. Water body-adjacent stations showed exceptionally high ungulate RAI (1,024.8), driven by concentrated detections of gaur and sambar at riparian sites. Agricultural land supported low overall wildlife RAI, with only ungulates (3.47) and carnivores (2.63) detected at appreciable rates in these habitats.

Table 5. Mean relative abundance index (RAI; detections per 100 trap-nights) by land-cover class and guild. Only guild–LULC combinations with detections are shown. Values reflect proximity-based assignment of stations to the nearest LULC polygon.

LULC class	Guild	Mean RAI	Records	Stations
Forests	Ungulate	35.45	502	136
Forests	Carnivore	8.99	491	130
Forests	Primate	3.65	41	35
Forests	Bird	3.64	93	44
Water Bodies	Ungulate	1,024.81	38	9
Water Bodies	Primate	64.99	5	5
Water Bodies	Carnivore	42.00	32	9
Shrubs	Ungulate	27.17	5	1
Agriculture	Ungulate	3.47	7	2
Agriculture	Carnivore	2.63	5	2

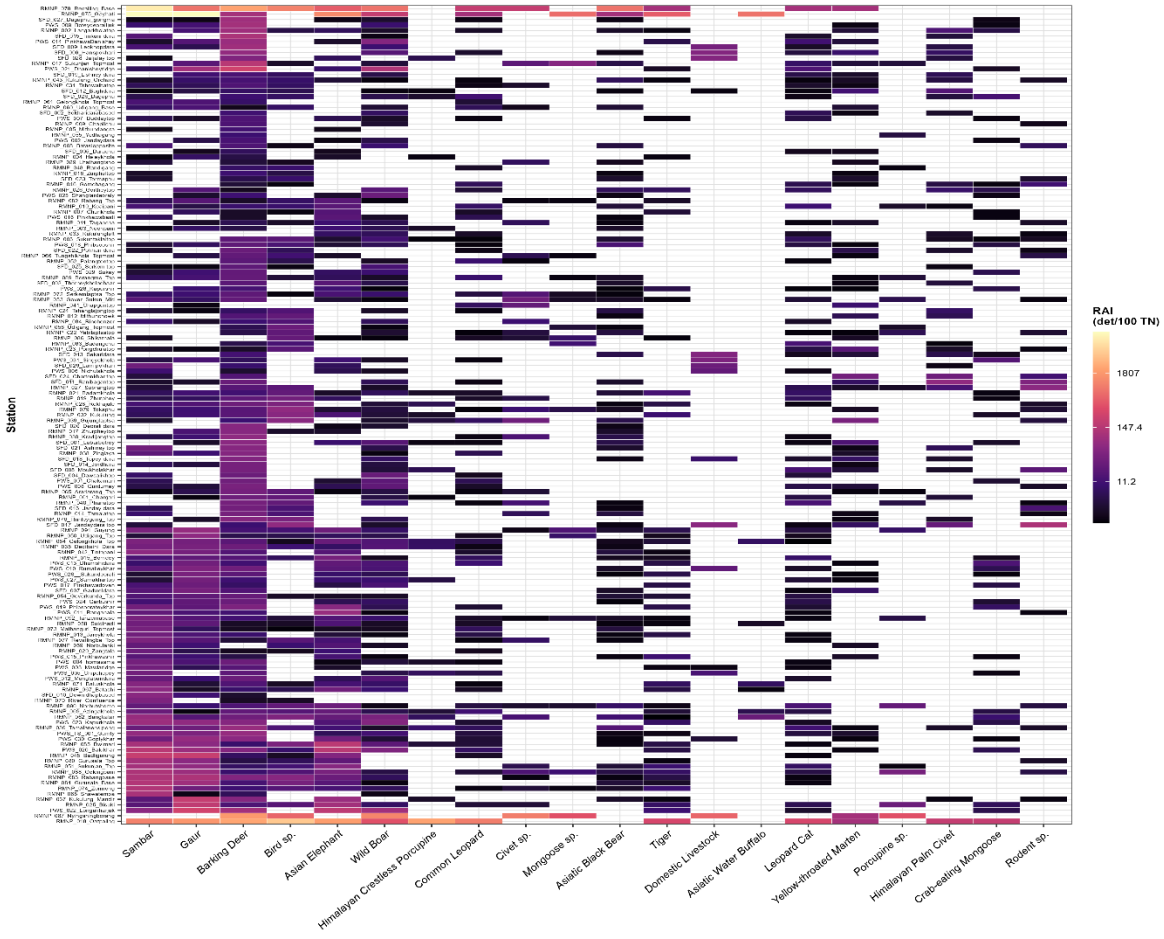

Figure 4. *Relative abundance index (RAI) heatmap showing the top 20 species across 149 stations, ordered by Ward hierarchical clustering. Rows represent species and columns represent stations. Colour intensity indicates RAI magnitude. Barking deer, sambar, and gaur*

dominate the community numerically, while large carnivores (tiger, leopard) show sparse but spatially structured detections.

Activity overlap structure

The 42 x 42 pairwise activity overlap matrix revealed strong within-guild temporal clustering (Figure 5). Ungulates showed consistently high Dhat4 values with each other (range: 0.75–0.94), reflecting shared crepuscular and diurnal activity patterns. Nocturnal species (civets, porcupines, leopard cat) formed a second temporal guild with high within-group overlap. Between-guild overlap was generally lower, particularly between strictly nocturnal civets and diurnal ungulates (Dhat4 range: 0.35–0.55), confirming that temporal partitioning contributes to community-level niche separation.

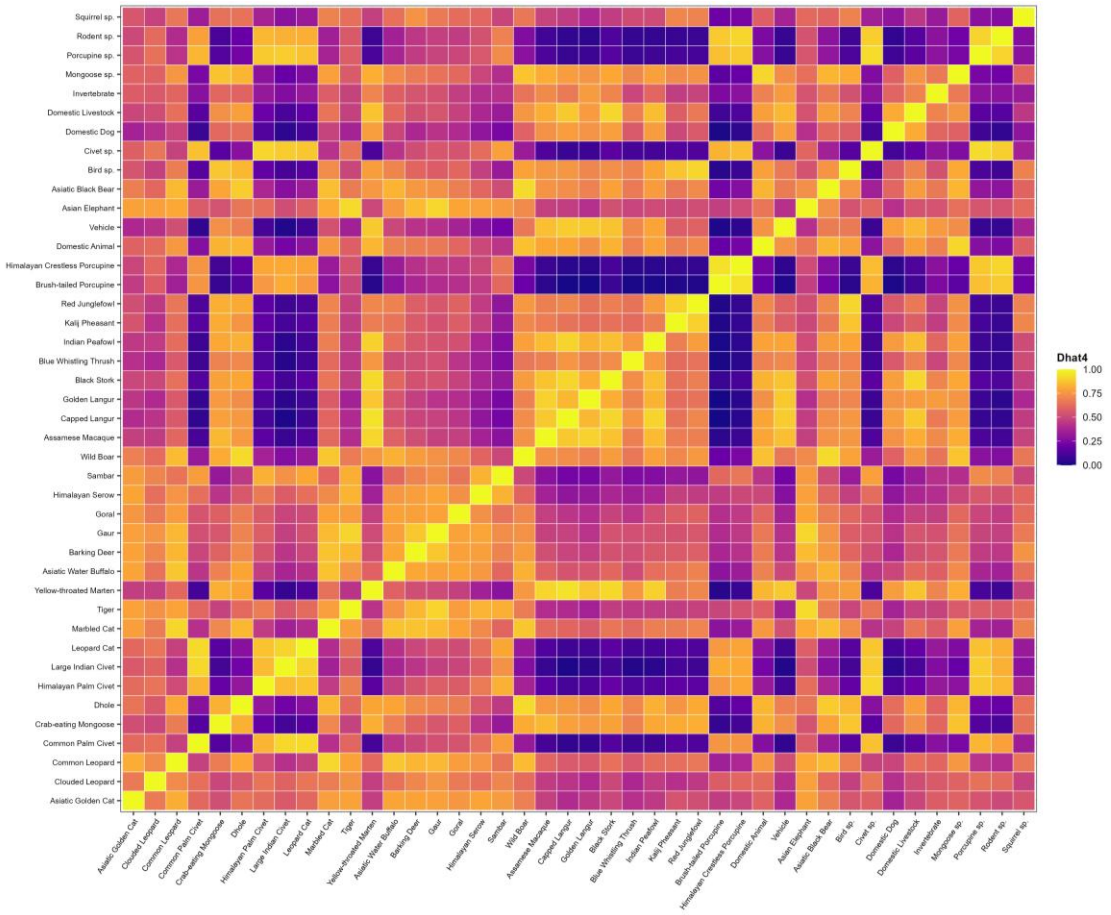

Figure 5. *Activity overlap heatmap showing pairwise Dhat4 coefficients among 42 species, ordered by guild. Warm colours indicate high temporal overlap; cool colours indicate temporal segregation. Within-guild overlap is generally high, while between-guild overlap (particularly nocturnal civets vs. diurnal ungulates) is low, indicating temporal niche partitioning at the community level.*

Climate–diversity relationships

Station-level species richness and total RAI showed significant relationships with climatic variables (Figure 6). Species richness increased across both the annual mean temperature gradient (bio1) and the precipitation-seasonality gradient (bio15), while total wildlife RAI

showed a weak positive relationship with annual precipitation (bio12). Stations receiving > 4,000 mm annual precipitation supported a mean of 12.3 species compared with 10.3 species at stations below 3,000 mm, and the highest precipitation-seasonality quartile supported a mean of 15.9 species compared with 10.9 species in the lowest quartile. Mean annual temperature showed a weak positive relationship with total RAI, reflecting the concentration of large-bodied, high-detection ungulates (gaur, sambar) at warmer low-elevation stations.

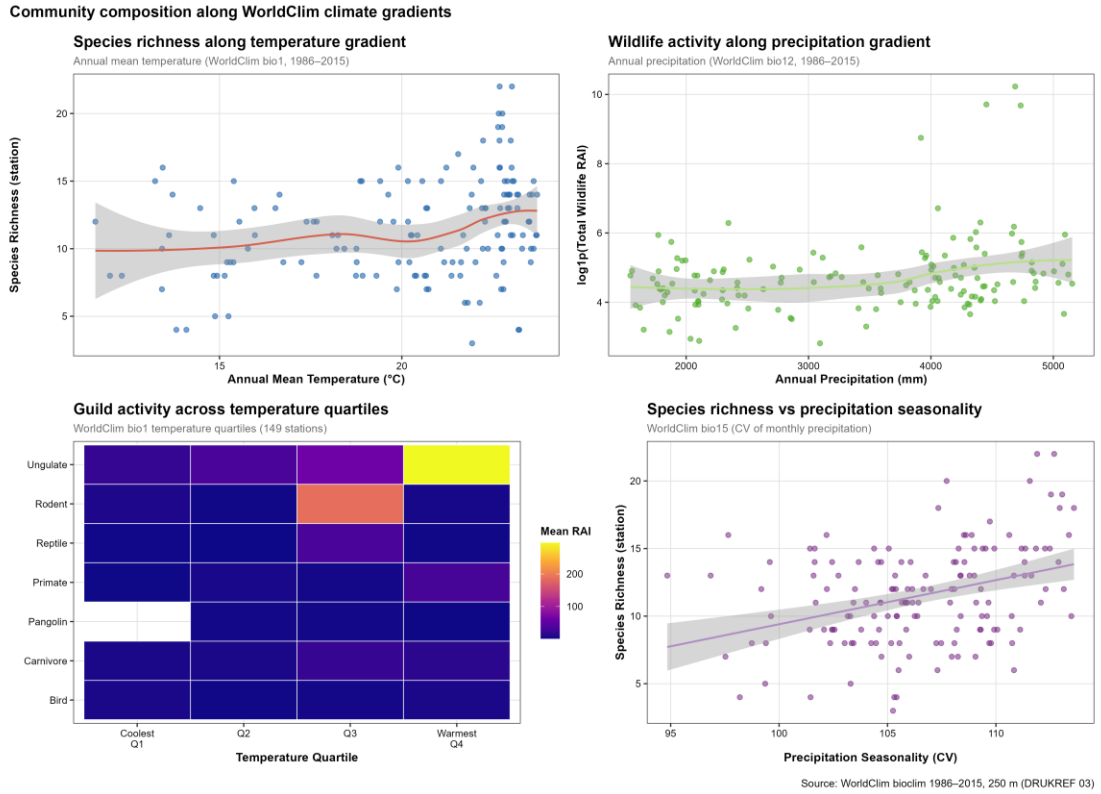

Figure 6. *Climate–diversity relationships across 149 stations. (a) Species richness versus annual mean temperature (bio1); (b) total wildlife RAI versus annual precipitation (bio12); (c) guild activity across temperature quartiles; (d) species richness versus precipitation seasonality (bio15). LOESS smoothers with 95% confidence bands are shown.*

Species accumulation and sampling adequacy

The randomised species accumulation curve continued to rise through the full survey, but flattened substantially beyond approximately 120 stations, reaching 73 species across all 149 stations (Figure 7). At the station level, Chao1 richness estimates ranged from 3.0 to 26.0 (mean = 17.3), suggesting that individual stations harbour an average of 3.9 undetected species beyond the observed mean of 13.4. The near-asymptotic accumulation curve and convergence of the Chao1 estimator confirm that the sampling design captured the large majority of the detectable mammalian community.

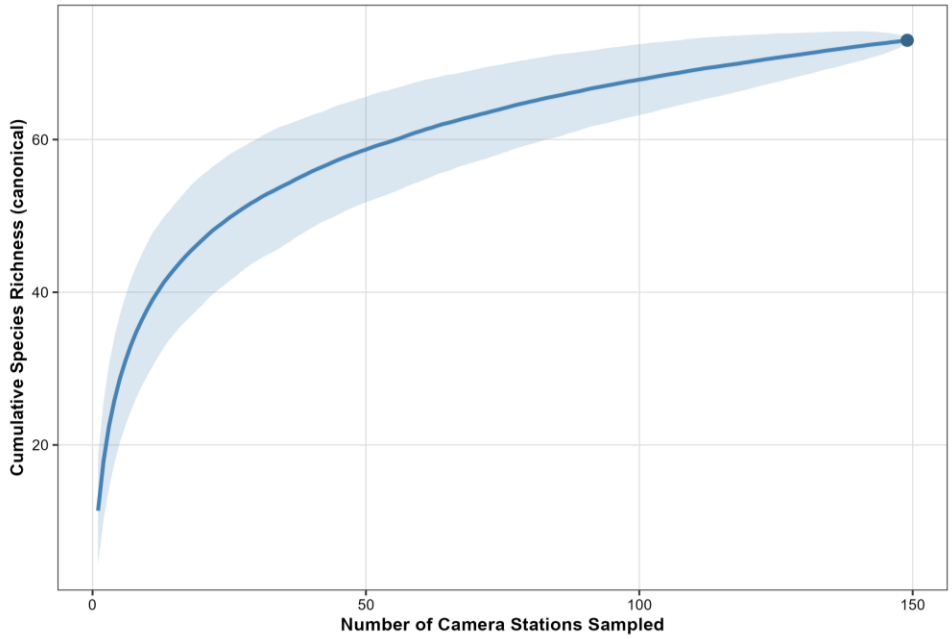

Figure 7. *Randomised species accumulation curve (1,000 permutations) showing cumulative species richness as a function of sampling effort (number of stations). The shaded area represents the 95% confidence interval. The curve flattens beyond approximately 120 stations and reaches 73 species by 149 stations, confirming adequate sampling coverage of the mammalian community.*

Mesopredator release

Correlations between tiger RAI and subordinate carnivore RAI provided no evidence of mesopredator release (Figure S1). Tiger–leopard RAI correlation was weakly negative and non-significant (r = -0.07, $p > 0.05$), indicating no spatial relationship between apex and subordinate large carnivore abundances. Tiger–dhole RAI correlation was marginally negative (r = -0.17, p = 0.084) but did not achieve conventional significance. These results suggest that competitive release of subordinate carnivores is not occurring at detectable levels in this landscape, consistent with the persistence of tigers at moderate densities sufficient to maintain top-down regulatory influence.

Phenological patterns

Monthly detection patterns revealed clear phenological structure in community activity (Figure S3). Ungulate detections peaked during the dry season (March–May), coinciding with reduced canopy cover and concentrated use of riparian water sources. Large carnivore detections were more evenly distributed across the 8-month survey window (February–September), though a modest increase in tiger detections during March–April coincided with the ungulate peak. The monsoon-adjacent period (June–August) showed reduced overall detection rates across guilds, reflecting both genuine behavioural shifts and reduced camera operability during heavy rainfall.

Discussion

Climate as the dominant assembly filter

Our results demonstrate that climatic gradients impose the strongest environmental filter on mammalian community composition in south-central Bhutan. Annual precipitation (bio12; r^2 = 0.366) and mean annual temperature (bio1; r^2 = 0.311) together explained more community-level variation than any disturbance-related variable, with their envfit vectors strongly aligned toward negative NMDS2 values. This finding aligns with macroecological studies showing that energy and water availability are primary determinants of mammalian diversity along elevational gradients (Chen et al., 2011; Blois et al., 2013). The strong coupling of temperature and precipitation along the Himalayan slope means that these variables act as a composite elevational filter, structuring community transitions from lowland subtropical assemblages (elephant, tiger, gaur) to montane temperate assemblages (marten, marbled cat, Himalayan palm civet).

The dominance of climate over disturbance as a community structuring force is notable given the conservation context. In more heavily modified landscapes, anthropogenic disturbance often emerges as the primary assembly filter, overriding climatic gradients through habitat loss and fragmentation (Newbold et al., 2015). The relatively weak but significant effect of road distance (r^2 = 0.052, p = 0.014) in our study suggests that disturbance is beginning to influence community composition but has not yet become the dominant force. This interpretation is consistent with Bhutan's high forest cover and relatively low road density within protected areas, and provides a baseline against which future disturbance impacts can be measured.

Co-occurrence patterns and biotic structuring

The identification of 214 significant co-occurrence pairs (21.6% of 990 tested) indicates substantial non-random spatial structure in the mammalian community. The predominance of positive associations (143 vs. 71 negative) is consistent with shared habitat responses driving most co-occurrence patterns, as species tracking the same environmental gradients tend to co-occur more frequently than expected. However, the presence of 71 significant negative associations after accounting for marginal occurrence probabilities suggests that competitive exclusion or predator avoidance may contribute to spatial segregation beyond what environmental filtering alone would produce.

The strongest positive associations involved species sharing lowland riparian habitats. The Asian elephant–tiger pair (SES = 6.14) exemplifies co-occurrence driven by shared preference for lowland forests and riparian corridors, rather than any direct facilitative interaction. Similarly, the strong association between masked palm civet and black stork (SES = 8.48), while statistically robust, likely reflects shared microhabitat use in moist lowland forests rather than a biotic interaction. These findings underscore the well-known challenge of distinguishing habitat-mediated co-occurrence from genuine biotic interactions using presence-absence data alone (Ovaskainen et al., 2017). The strongest negative associations were more ecologically informative. The segregation between Asian elephant and highland species (marbled cat, SES = -4.37; Himalayan palm civet, SES = -4.63; yellow-throated marten, SES = -3.34) clearly reflects elevational habitat segregation. More intriguingly, the negative associations between closely related species groups (Himalayan palm civet–civet sp., SES = -3.60; common palm civet–civet sp., SES = -3.28) may indicate competitive exclusion within the viverrid guild, though taxonomic uncertainty in the "civet sp." category complicates this interpretation.

Station clustering along a continuous gradient

The low silhouette width (0.128) for the optimal two-cluster partition indicates that community composition varies along a continuous gradient rather than forming discrete assemblage types. This is ecologically expected along elevational transects where environmental conditions change gradually. The cluster partition should therefore be interpreted as a heuristic division of a continuous gradient rather than evidence for distinct community types (Legendre & Legendre, 2012).

Despite this caveat, the indicator species for each cluster are biologically meaningful. The highland cluster (yellow-throated marten, Himalayan palm civet, marbled cat) comprises species associated with cool, moist montane forests with dense canopy cover. The lowland cluster (Asian elephant, tiger, common palm civet) includes the megafauna that dominates subtropical and tropical lowland assemblages across South Asia. This elevational turnover in mammalian community composition has been documented in other Himalayan landscapes (Penjor et al., 2021) and reflects the broad biogeographic transition from Indo-Malayan lowland fauna to Sino-Himalayan montane fauna along the southern slopes of the eastern Himalayas.

Guild-specific responses

The disproportionately high ungulate RAI at water body-adjacent stations (mean RAI = 1,024.8) highlights the critical importance of riparian habitats for large herbivores in this landscape. Gaur and sambar concentrate at water sources during the dry season, creating localised hotspots of ungulate biomass that likely attract predators and influence predator–prey encounter dynamics. The low overall wildlife RAI in agricultural land suggests that crop cultivation creates a habitat barrier for most wild species, although the limited number of agricultural stations (n = 2) constrains inference.

Carnivore detection rates were highest in forests (mean RAI = 8.99) and water body-adjacent habitats (42.00), consistent with their dependence on intact forest cover and the prey concentrations associated with riparian zones. The lower carnivore RAI in agricultural land (2.63) relative to forests suggests avoidance of human-dominated habitats, although the small sample size prevents robust generalisation.

Absence of mesopredator release

The lack of significant negative correlations between tiger and subordinate carnivore RAI (tiger–leopard r = -0.07; tiger–dhole r = -0.17) provides no support for the mesopredator release hypothesis in this landscape. This null result is consistent with the expectation that mesopredator release requires substantial reduction in apex predator populations (Prugh et al., 2009; Ritchie & Johnson, 2009). In south-central Bhutan, tigers persist at moderate densities across 34% of survey stations, suggesting that top-down regulatory influence remains ecologically effective. The marginally negative tiger–dhole correlation (p = 0.084) may reflect weak interference competition or spatial partitioning between these two large carnivores, but does not constitute evidence of competitive release.

This finding contrasts with documented mesopredator release in landscapes where large carnivores have been extirpated or severely reduced (Soule et al., 1988). The persistence of the full carnivore guild in south-central Bhutan – including tiger, leopard, dhole, clouded leopard, and multiple small carnivore species – makes this landscape valuable as a reference condition for understanding community dynamics in the absence of apex predator loss.

Temporal niche partitioning

The activity overlap matrix revealed clear temporal guild structure, with diurnal-crepuscular ungulates, nocturnal civets and small carnivores, and cathemeral large carnivores occupying partially segregated temporal niches. This temporal partitioning likely reduces interspecific encounter rates and contributes to the coexistence of ecologically similar species. The high within-guild overlap among ungulates (Dhat4 > 0.75) suggests that temporal partitioning is more important between guilds than within them, consistent with studies showing that body-size-mediated spatial partitioning is the primary niche axis within ungulate guilds (Karanth & Sunquist, 1995).

NMDS stress and methodological considerations

The NMDS stress value of 0.208 falls slightly above the conventional threshold of 0.20 considered "good" by Clarke (1993), though well below the 0.30 threshold for "poor" representations. This stress level is typical for community datasets with high species richness and spatially heterogeneous composition, where perfect low-dimensional representation is inherently difficult. The stress value which is computed independently of the ordination, provide corroborating evidence for the environmental relationships identified.

The strong association between trap-nights and NMDS axes (r^2 = 0.369) warrants cautious interpretation. Stations with longer deployments detected more species, potentially inflating RAI at high-effort stations. This is addressed by using RAI (effort-standardised) rather than raw detection counts in the community matrix but acknowledge that residual effort effects may persist due to the non-linear relationship between sampling effort and detection probability.

Conservation implications

The dominance of climate gradients in structuring community composition underscores the importance of maintaining elevational connectivity within Bhutan's protected area network. As climate change shifts temperature and precipitation isoclines upslope, species tracking their climatic niche will require continuous forest corridors spanning the full elevational gradient. The RMNP–PWS–SFD corridor currently provides this connectivity, and its maintenance should be a conservation priority.

The weak but significant disturbance signal from road distance suggests that road development within or adjacent to protected areas may begin to reshape community composition if expanded. Monitoring community-level indicators (NMDS scores, cluster membership, indicator species abundances) along existing and proposed road corridors would provide early warning of disturbance-driven assembly shifts. The persistence of the complete large carnivore guild, and the absence of mesopredator release, indicates that this landscape retains ecological functionality at the apex of the trophic web. Conservation strategies should prioritise maintaining tiger populations at current or higher densities to preserve these top-down regulatory effects on community structure.

Limitations

Several limitations should be considered when interpreting these results. First, the single-year survey (2022) captures a snapshot of community composition that may not reflect inter-annual variation driven by climatic fluctuations, prey population dynamics, or episodic disturbance events. Multi-year surveys would enable assessment of temporal stability in community structure and more robust estimation of rare species occurrence.

Second, RAI assumes proportionality between detection rate and true abundance, an assumption that may not hold across species with different body sizes, movement rates, and detection probabilities (Sollmann, 2018). Species-specific detection probability correction, for example through occupancy modelling or N-mixture models, would strengthen abundance-based inference but was beyond the scope of this community-level analysis. Third, the co-occurrence null model, while widely used, cannot definitively distinguish biotic interactions from fine-scale environmental heterogeneity not captured by the measured covariates. Joint species distribution models (JSDMs) that simultaneously estimate species-specific environmental responses and residual species correlations (Warton et al., 2015; Ovaskainen et al., 2017) would provide a more rigorous framework for separating these effects, and are a priority for future analysis.

Fourth, the low silhouette width (0.128) for station clustering indicates that discrete community types are not well-supported. The two-cluster partition should be interpreted as a heuristic summary of a continuous gradient rather than evidence for distinct assemblage types. Fifth, the 42-species community matrix includes species at the threshold of adequate detection (5 stations minimum), and the inclusion or exclusion of rare species can influence ordination results. Sensitivity analyses with a 10-station minimum threshold yielded qualitatively similar patterns but are not presented here.

Conclusion

This study demonstrates that mammalian community assembly in south-central Bhutan is primarily structured by climatic gradients operating along the Himalayan elevational transect, with anthropogenic disturbance exerting a secondary but detectable filtering effect. The identification of 214 significant co-occurrence pairs, predominantly positive, suggests that shared habitat responses dominate community spatial structure, while the 71 negative associations point to competitive or segregative interactions that warrant further investigation with joint species distribution modelling approaches. The continuous rather than discrete nature of community turnover along the gradient emphasises the importance of maintaining landscape connectivity across the full elevational range.

The absence of mesopredator release in a landscape retaining its complete carnivore guild provides a valuable reference condition for understanding trophic dynamics in intact Himalayan ecosystems. As development pressures intensify in Bhutan's southern foothills, the community-level baselines established here – NMDS ordination structure, co-occurrence architecture, guild-specific habitat associations, and temporal niche partitioning – will serve as benchmarks against which future changes in community assembly processes can be evaluated.

Data Availability

All data and analytical code supporting this study are archived in the project repository at https://github.com/wangdiues/camtrap_ecology_analytics. The reproducible pipeline includes all camera-trap processing scripts, community analysis code, figure generation scripts, and package dependency files. Raw camera-trap images are available upon reasonable request to the Department of Forests and Park Services, Royal Government of Bhutan.

Author Contributions

All authors contributed to study design, field logistics, data collection, analysis, interpretation, and manuscript revision. The lead author conceived the study, conducted fieldwork, processed camera-trap data, performed all analyses, and drafted the manuscript. All authors approved the final version.

Acknowledgements

Authors thank the Department of Forests and Park Services, Royal Government of Bhutan, for research permits and support. Authors are grateful to staff of Royal Manas National Park, Phipsoo Wildlife Sanctuary, and Sarpang Forest Division for field support. Camera-trap equipment was provided through project resources and institutional support. This research was conducted under institutional ethics approval.

References

Ahumada, J.A., Silva, C.E.F., Gajapersad, K., Hallam, C., Hurtado, J., Martin, E., McWilliam, A., Mugerwa, B., O'Brien, T., Rovero, F., Sheil, D., Spironello, W.R., Winarni, N. & Andelman, S.J. (2011). Community structure and diversity of tropical forest mammals: data from a global camera trap network. *Philosophical Transactions of the Royal Society B*, 366, 2703–2711.

Benitez-Lopez, A., Alkemade, R. & Verweij, P.A. (2010). The impacts of roads and other infrastructure on mammal and bird populations: a meta-analysis. *Biological Conservation*, 143, 1307–1316.

Blanchet, F.G., Cazelles, K. & Gravel, D. (2020). Co-occurrence is not evidence of ecological interactions. *Ecology Letters*, 23, 1050–1063.

Blois, J.L., Zarnetske, P.L., Fitzpatrick, M.C. & Finnegan, S. (2013). Climate change and the past, present, and future of biotic interactions. *Science*, 341, 499–504.

Cardillo, M., Mace, G.M., Jones, K.E., Bielby, J., Bininda-Emonds, O.R.P., Sechrest, W., Orme, C.D.L. & Purvis, A. (2005). Multiple causes of high extinction risk in large mammal species. *Science*, 309, 1239–1241.

Cavender-Bares, J., Kozak, K.H., Fine, P.V.A. & Kembel, S.W. (2009). The merging of community ecology and phylogenetic biology. *Ecology Letters*, 12, 693–715.

Chao, A. (1984). Nonparametric estimation of the number of classes in a population. *Scandinavian Journal of Statistics*, 11, 265–270.

Chen, I.C., Hill, J.K., Ohlemuller, R., Roy, D.B. & Thomas, C.D. (2011). Rapid range shifts of species associated with high levels of climate warming. *Science*, 333, 1024–1026.

Clarke, K.R. (1993). Non-parametric multivariate analyses of changes in community structure. *Australian Journal of Ecology*, 18, 117–143.

Colwell, R.K., Chao, A., Gotelli, N.J., Lin, S.Y., Mao, C.X., Chazdon, R.L. & Longino, J.T. (2012). Models and estimators linking individual-based and sample-based rarefaction, extrapolation and comparison of assemblages. *Journal of Plant Ecology*, 5, 3–21.

Cribari-Neto, F. & Zeileis, A. (2010). Beta regression in R. *Journal of Statistical Software*, 34, 1–24.

De Caceres, M. & Legendre, P. (2009). Associations between species and groups of sites: indices and statistical inference. *Ecology*, 90, 3566–3574.

Dufrene, M. & Legendre, P. (1997). Species assemblages and indicator species: the need for a flexible asymmetrical approach. *Ecological Monographs*, 67, 345–366.

Fick, S.E. & Hijmans, R.J. (2017). WorldClim 2: new 1-km spatial resolution climate surfaces for global land areas. *International Journal of Climatology*, 37, 4302–4315.

Gotelli, N.J. (2000). Null model analysis of species co-occurrence patterns. *Ecology*, 81, 2606–2621.

Gotelli, N.J. & Colwell, R.K. (2001). Quantifying biodiversity: procedures and pitfalls in the measurement and comparison of species richness. *Ecology Letters*, 4, 379–391.

HilleRisLambers, J., Adler, P.B., Harpole, W.S., Levine, J.M. & Mayfield, M.M. (2012). Rethinking community assembly through the lens of coexistence theory. *Annual Review of Ecology, Evolution, and Systematics*, 43, 227–248.

Kraft, N.J.B., Adler, P.B., Godoy, O., James, E.C., Fuller, S. & Levine, J.M. (2015). Community assembly, coexistence and the environmental filtering metaphor. *Functional Ecology*, 29, 592–599.

Legendre, P. & Legendre, L. (2012). *Numerical Ecology*, 3rd edn. Elsevier, Amsterdam.

Meek, P.D., Ballard, G.A., Claridge, A., Kays, R., Moseby, K., O'Brien, T., O'Connell, A., Sanderson, J., Swann, D.E., Tobler, M. & Townsend, S. (2014). Recommended guiding principles for reporting on camera trapping research. *Biodiversity and Conservation*, 23, 2321–2343.

Meredith, M. & Ridout, M. (2014). overlap: Estimates of coefficient of overlapping for animal activity patterns. R package version 0.3.2.

Newbold, T., Hudson, L.N., Hill, S.L.L., Contu, S., Lysenko, I., Senior, R.A., Borger, L., Bennett, D.J., Choimes, A., Collen, B., Day, J., De Palma, A., Diaz, S., Echeverria-Londono, S., Edgar, M.J., Feldman, A., Garon, M., Harrison, M.L.K., Alhusseini, T., Ingram, D.J., Itescu, Y., Kattge, J., Kemp, V., Kirkpatrick, L., Kleyer, M., Correia, D.L.P., Martin, C.D., Meiri, S., Novosolov, M., Pan, Y., Phillips, H.R.P., Purve, D.W., Robinson, A., Simpson, J., Tuck, S.L.,

Weiher, E., White, H.J., Ewers, R.M., Mace, G.M., Scharlemann, J.P.W. & Purvis, A. (2015). Global effects of land use on local terrestrial biodiversity. *Nature*, 520, 45–50.

O'Brien, T.G., Kinnaird, M.F. & Wibisono, H.T. (2003). Crouching tigers, hidden prey: Sumatran tiger and prey populations in a tropical forest landscape. *Animal Conservation*, 6, 131–139.

Oksanen, J., Simpson, G.L., Blanchet, F.G., Kindt, R., Legendre, P., Minchin, P.R., O'Hara, R.B., Solymos, P., Stevens, M.H.H., Szoecs, E., Wagner, H., Barbour, M., Bedward, M., Bolker, B., Borcard, D., Carvalho, G., Chirico, M., De Caceres, M., Durand, S., Evangelista, H.B.A., FitzJohn, R., Friendly, M., Furneaux, B., Hannigan, G., Hill, M.O., Lahti, L., McGlinn, D., Ouellette, M.H., Ribeiro Cunha, E., Smith, T., Stier, A., Ter Braak, C.J.F. & Weedon, J. (2022). vegan: Community Ecology Package. R package version 2.6-4.

Ovaskainen, O., Tikhonov, G., Norberg, A., Guillaume Blanchet, F., Duan, L., Dunson, D., Roslin, T. & Abrego, N. (2017). How to make more out of community data? A conceptual framework and its implementation as models and software. *Ecology Letters*, 20, 561–576.

Pebesma, E. (2018). Simple features for R: standardized support for spatial vector data. *The R Journal*, 10, 439–446.

Penjor, U., Wangdi, S., Tandin, T. & Macdonald, D.W. (2021). Estimating the density of tiger and co-occurring prey species using spatial capture-recapture models in Bhutan. *Journal of Zoology*, 313, 131–142.

Prugh, L.R., Stoner, C.J., Epps, C.W., Bean, W.T., Ripple, W.J., Laliberte, A.S. & Brashares, J.S. (2009). The rise of the mesopredator. *BioScience*, 59, 779–791.

Ridout, M.S. & Linkie, M. (2009). Estimating overlap of daily activity patterns from camera trap data. *Journal of Agricultural, Biological, and Environmental Statistics*, 14, 322–337.

Ripple, W.J., Estes, J.A., Beschta, R.L., Wilmers, C.C., Ritchie, E.G., Hebblewhite, M., Berger, J., Elmhagen, B., Letnic, M., Nelson, M.P., Schmitz, O.J., Smith, D.W., Wallach, A.D. & Wirsing, A.J. (2014). Status and ecological effects of the world's largest carnivores. *Science*, 343, 1241484.

Ritchie, E.G. & Johnson, C.N. (2009). Predator interactions, mesopredator release and biodiversity conservation. *Ecology Letters*, 12, 982–998.

Rovero, F., Martin, E., Rosa, M., Ahumada, J.A. & Spitale, D. (2014). Estimating species richness and modelling habitat preferences of tropical forest mammals from camera trap data. *PLoS ONE*, 9, e103300.

Sollmann, R. (2018). A gentle introduction to camera-trap data analysis. *African Journal of Ecology*, 56, 740–749.

Soule, M.E., Bolger, D.T., Alberts, A.C., Wright, J., Sorice, M. & Hill, S. (1988). Reconstructed dynamics of rapid extinctions of chaparral-requiring birds in urban habitat islands. *Conservation Biology*, 2, 75–92.

Tempa, T., Hebblewhite, M., Goldberg, J.F., Norbu, N., Wangchuk, T.R., Xiao, W. & Mills, L.S. (2019). The spatial distribution and population density of tigers in mountainous terrain of Bhutan. *Biological Conservation*, 238, 108192.

Tobler, M.W., Carrillo-Percastegui, S.E., Leite Pitman, R., Mares, R. & Powell, G. (2008). An evaluation of camera traps for inventorying large- and medium-sized terrestrial rainforest mammals. *Animal Conservation*, 11, 169–178.

Veech, J.A. (2013). A probabilistic model for analysing species co-occurrence. *Global Ecology and Biogeography*, 22, 252–260.

Wang, S.W., Lassoie, J.P. & Curtis, P.D. (2015). Farmer attitudes towards conservation in Jigme Singye Wangchuck National Park, Bhutan. *Environmental Conservation*, 33, 148–156.

Warton, D.I., Blanchet, F.G., O'Hara, R.B., Ovaskainen, O., Taskinen, S., Walker, S.C. & Hui, F.K.C. (2015). So many variables: joint modeling in community ecology. *Trends in Ecology & Evolution*, 30, 766–779.

Supporting Information

Supplementary figures are embedded below so the submission package remains self-contained.

Figure S1. Mesopredator release scatterplots.

(a) Tiger vs common leopard.

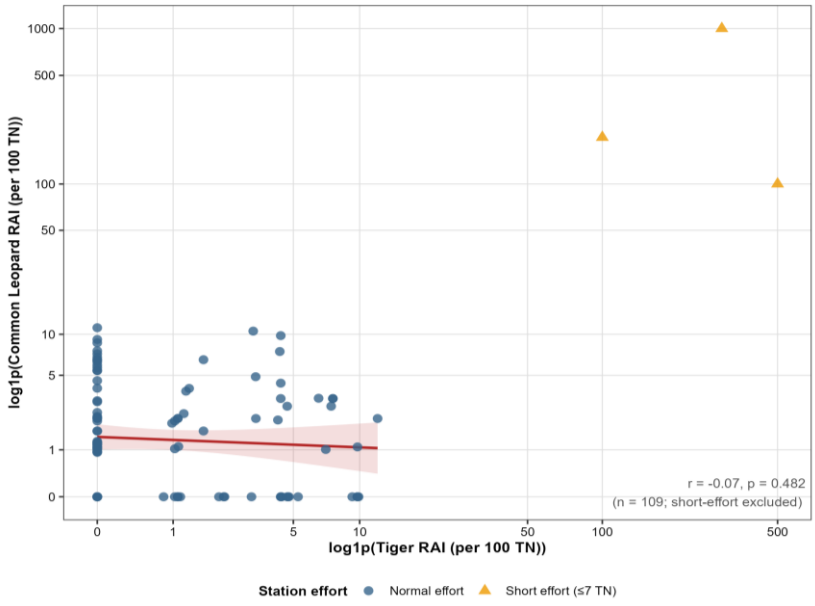

Figure S1a. *Tiger versus common leopard RAI by station.*

(b) Tiger vs dhole.

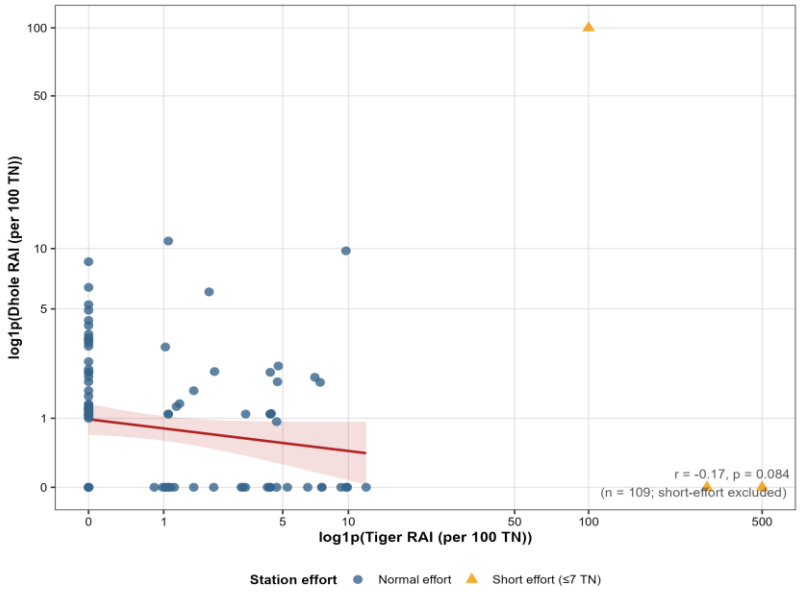

Figure S1b. *Tiger versus Dhole RAI by station.*

Figure S2. Guild-by-LULC RAI barplot.

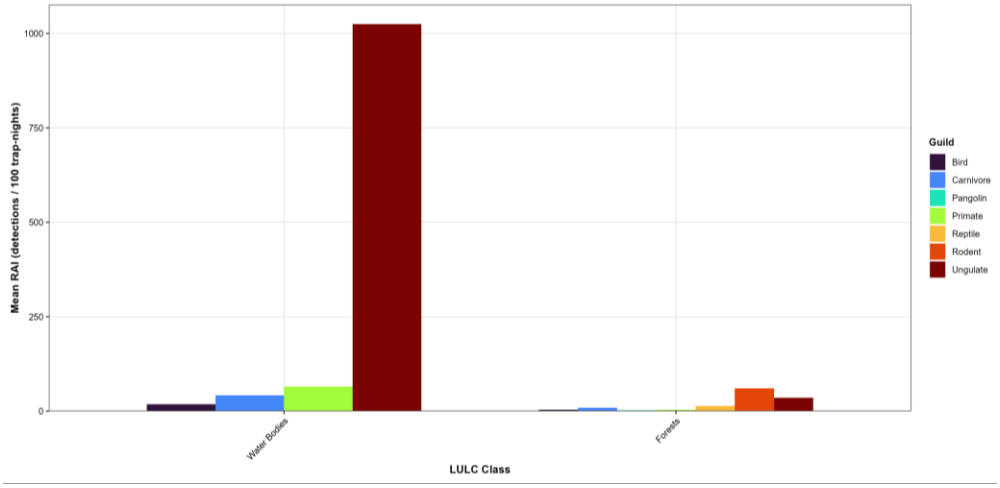

Figure S2. *Mean relative abundance index by land-cover class and species guild.*

Figure S3. Phenological heatmap.

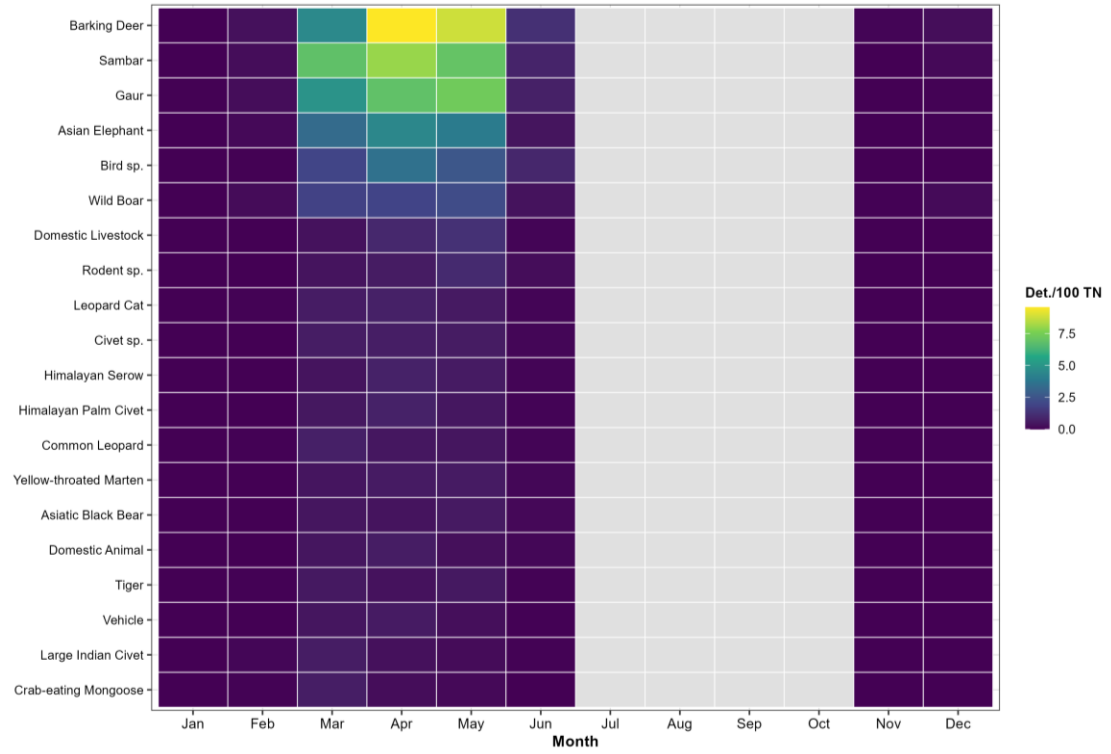

Figure S3. *Monthly detection heatmap for the top 20 species.*

Figure S4. Mesopredator activity overlap comparison.

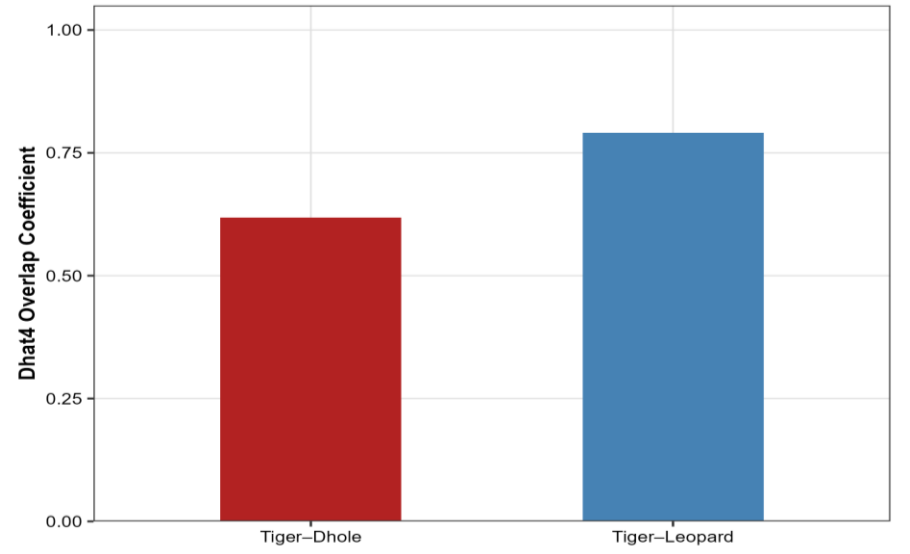

Figure S4. *Dhat4 overlap comparison for tiger versus mesopredators.*